Aust. J. Phys., 1991, **44**, 693–704

Imperfect Crystals and Dynamical X-ray Diffraction in the Complex Reflectance Plane

T. J. Davis

Division of Materials Science and Technology, CSIRO,
Locked Bag 33, Clayton, Vic. 3168, Australia.

Abstract

A theoretical framework is developed to describe the dynamical diffraction of X-rays in perfect and imperfect crystals. The propagation of the X-ray beam inside the crystal is described by the evolution of a set of trajectories in the complex reflectance plane. The trajectory path is determined from a form of the Takagi–Taupin equations and leads naturally to simple forms for the crystal reflectivity for perfect crystals. A stochastic model for the effects of crystal defects is developed in terms of the Langevin equation which leads to a description of diffraction from imperfect crystals as the evolution of densities in a parameter space, described by a Fokker–Planck equation.

1. Introduction

The effect of imperfections on the diffraction of X-rays in crystals is to introduce a degree of randomisation of the phases of the diffracted waves. Invariably, the study of diffraction from such crystals requires methods for calculating the collective effects of these phases, averaged over an ensemble of imperfect crystals (e.g. Dederichs 1971; Kato 1980, 1991; Holy 1982; Holy and Gabrielyan 1987; Becker and Al Haddad 1988).

Rather than follow this approach, the aim of this paper is to treat the phases of the X-rays indirectly by describing the behaviour of the complex reflectance as a function of position in the crystal. The state of the X-rays in each crystal, comprising a part of a statistical ensemble, will be represented by a point in the complex reflectance plane. A study of the effects of lattice distortions and defects on the trajectories of these points will lead to a statistical model and a Fokker–Planck equation governing the evolution of densities in a parameter space. This provides a theoretical framework for the description of X-ray diffraction in imperfect crystals.

The present work is directed towards Bragg reflections from extended face crystals and in particular, epilayers, where the crystal is considered to be statistically homogeneous in strata parallel to the crystal surface. In Section 2 the concept of an X-ray trajectory in the complex reflectance plane is developed, followed in Section 3 by a study of the effects of imperfections on the trajectories. This leads to the concept of a density of trajectories, the development of a stochastic defect model in Section 4, and finally, in Section 5, the evolution equation for these densities.

0004-9506/91/060693$05.00

2. Crystal Reflectance in the Complex Plane

The Takagi–Taupin equations (Takagi 1962, 1969; Taupin 1964) describe the variation with position in the crystal of the amplitudes of the transmitted and diffracted waves. These variations occur in the propagation directions of the X-ray beams. Consider a single, extended face crystal which is homogeneous in each plane parallel to the crystal surface so that the propagation directions can be projected onto the one axis and the equations written as functions only of depth t below the crystal surface. Here the origin of the coordinates will be at some point within the crystal (e.g. the boundary between a substrate and an epilayer) and t will be taken as positive in the direction of the crystal surface. It is assumed that the X-rays are plane waves. By defining the crystal reflectance $R(t)$ at depth t as the ratio of the diffracted and transmitted wave amplitudes at t, a first order differential equation for the crystal reflectance can be derived,

$$\mathrm{d}R/\mathrm{d}t = \mathrm{i}\alpha(\chi_h - 2\beta R + \chi_{-h} R^2). \tag{1}$$

Here $\alpha = -\pi k/\gamma_h$ with the X-ray wavelength given by $1/k = \lambda$; γ_0 and γ_h are the direction cosines of the transmitted and diffracted waves with respect to the crystal surface normal; χ'_h and χ'_{-h} are the Fourier components associated with the reciprocal lattice vectors $\boldsymbol{h}$ and $-\boldsymbol{h}$ of the dielectric susceptibility of the crystal, with $\chi_h = C\chi'_h$ and $\chi_{-h} = -C(\gamma_h/\gamma_0)\chi'_{-h}$, where C is the polarisation factor; and β is the resonance parameter given by

$$\beta = n^2 \frac{k_h^2 - k^2}{2k^2} - n \frac{\hat{\boldsymbol{k}}_h \cdot \nabla(\boldsymbol{h} \cdot \boldsymbol{\nu}(\xi))}{k} = \bar{\beta} + \beta_\xi . \tag{2}$$

In this equation $n = (1+\chi_0)^{1/2}$ is the refractive index for X-rays, $\boldsymbol{k}$ and $\boldsymbol{k}_h$ the wavevectors of the transmitted and diffracted waves in the crystal interior with $\boldsymbol{k}_h = \boldsymbol{k}+\boldsymbol{h}$, and $\boldsymbol{\nu}$ the displacement of each point in the lattice from its normal position due to strain in the crystal. The parameter ξ represents a random quantity and it will be used in the description of the imperfect lattice, as discussed below.

Note that the resonance parameter has been separated into two components. The first component is a function of the angle of incidence of the X-ray beam while the second component depends on the state of strain in the crystal.

The reflectance is a complex quantity, the phase of which is the phase difference between the transmitted and diffracted waves in the crystal. Rather than focus on the direct form of the reflectance as a function of position, consider the complex reflectance plane with axes defined by $(x, y) = (\mathrm{Re}\, R, \mathrm{Im}\, R)$. Equation (1) then describes the 'motion' of a point located at $\big(x(t), y(t)\big)$ as a function of t. At each position in the crystal, the X-ray beam is associated with a particular reflectance, which is represented by a point in the complex reflectance plane. Because the reflectance is a function of position t, the location of a point in the complex plane changes as t is varied. By tracing out the path followed by the point, a trajectory in the complex plane is described (Fig. 1). This trajectory describes the relative phase and the amplitudes of the X-rays in the crystal as a function of depth. Here the depth t now plays the

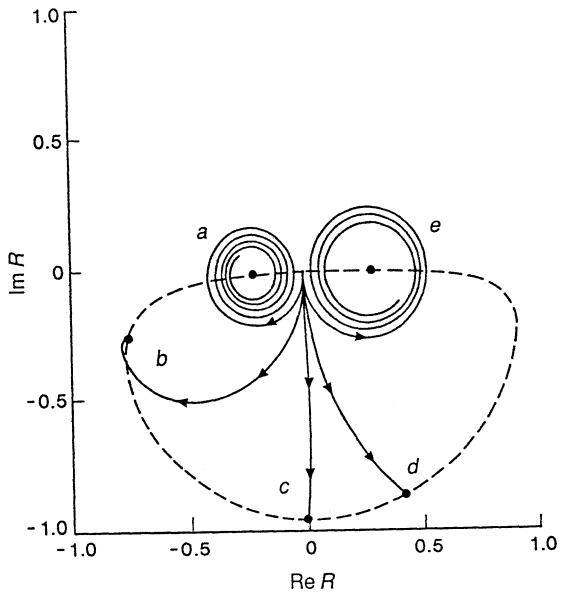

Fig. 1. Trajectories in the complex reflectance plane for a 10 μm thick silicon 111 wafer determined at a number of incident angles. The angles are measured in arcseconds relative to the Bragg angle: (*a*) 9″, (*b*) 4″, (*c*) 0, (*d*) −1″ and (*e*) −6″. The dashed curve is the locus of the singularities for all angles of incidence. The X-ray wavelength was 0·154 nm.

part of a time-like parameter and for constant coefficients it can be eliminated altogether from the equations of 'motion':

$$\begin{aligned} \mathrm{d}y/\mathrm{d}x &= (\mathrm{d}y/\mathrm{d}t)\,(\mathrm{d}x/\mathrm{d}t)^{-1} \\ &= \frac{\mathrm{Im\,i}\left(\chi_h - 2\beta(x+\mathrm{i}y) + \chi_{-h}(x+\mathrm{i}y)^2\right)}{\mathrm{Re\,i}\left(\chi_h - 2\beta(x+\mathrm{i}y) + \chi_{-h}(x+\mathrm{i}y)^2\right)}. \end{aligned} \tag{3}$$

This is an equation for the tangent to the trajectory (i.e. the trajectory direction) in the complex plane. The tangent becomes undefined when both the numerator and the denominator are zero, which occurs when the complex number R_0 satisfies

$$\chi_{-h} R_0^2 - 2\beta R_0 + \chi_h = 0, \tag{4}$$

and it is given by

$$R_0(\beta) = \{\beta \pm (\beta^2 - \chi_h \chi_{-h})^{1/2}\}/\chi_{-h} = (\beta + \omega)/\chi_{-h}. \tag{5}$$

This is a singular point of the trajectory and it depends on the incident angle of the transmitted beam, through β. An analysis of the behaviour of the trajectory in the vicinity of $R_0(\beta)$ shows that the singular point is a stable focus of the system (Bogoliubov and Mitropolsky 1962; Brand 1966) with all trajectories for a given β asymptoting to this value. This fact identifies

$R_0(\beta)$ as the reflectance of an infinitely thick perfect crystal and, as such, the sign of ω is chosen to ensure that $|R| < 1$. In Fig. 1 the locus of points $\left(\mathrm{Re}\, R_0(\beta), \mathrm{Im}\, R_0(\beta)\right)$ is plotted as the angle of incidence of the X-rays (and hence β) is varied.

Since all trajectories for a given β spiral around the singular point, the solution to (1) takes a simpler form when expressed relative to R_0. Using equations (4) and (5) to eliminate χ_h and β from (1) and assuming that R_0 is constant yields

$$\frac{\mathrm{d}(R-R_0)}{\mathrm{d}t} = \mathrm{i}\,\alpha(R-R_0)\{2\omega + \chi_{-h}(R-R_0)\}. \tag{6}$$

With the boundary condition $R(t{=}0) = 0$ the solution to equation (6) is

$$R = R_0\{1 - \exp(2\mathrm{i}\,\alpha\omega t)\}\frac{1 - R_0\chi_{-h}/2\omega}{1 - (R_0\chi_{-h}/2\omega)\{1 - \exp(2\mathrm{i}\,\alpha\omega t)\}}. \tag{7}$$

This is the reflectance as a function of t for a perfect crystal, based on dynamical diffraction theory. The real part of ω determines the angular frequency of the trajectory about the singular point while the imaginary part, related to the absorption of X-rays, determines the rate at which the trajectory approaches the singularity. Close to the Bragg peak, ω is very small and the trajectory is modified by the denominator in (7) causing it to approach R_0 much faster than would be dictated by $\mathrm{Im}\,\omega$. This is also seen in (6) when the nonlinear term dominates and the subsequent solution shows that $R \to R_0$ as $1/t$. In kinematic descriptions of diffraction [obtained by setting $\chi_{-h} = 0$ in (1)], this effect is absent leading to large errors near the Bragg peak. The reflectivity, $R(t)^*R(t)$, is the square of the distance from the origin to the point on the trajectory corresponding to depth t. This distance is seen to oscillate with depth (the Pendellosüng effect).

3. Imperfect Crystal Trajectories

In this section the effects on the trajectories in the complex reflectance plane of imperfections in the crystal lattice are discussed. Here, a large ensemble of the single crystals treated in Section 2 will be considered. The composition of each crystal may vary with depth but it is assumed that the crystal remains homogeneous in each plane parallel to the crystal surface. This assumption is equivalent to ignoring the boundaries between adjacent crystallites in each plane. The state of diffraction within each crystal will be represented by a corresponding point in the complex plane. If all the crystals are identical, then all the points will coincide and will follow the same trajectory. Any variation in the crystals will result in the points being distributed over the complex plane. The ultimate aim (Section 5) will be to derive a single equation describing the response of the ensemble to the X-ray beam.

There are two classes of imperfections that will be discussed, albeit in an idealised fashion. These are (i) idealised point defects and (ii) extended defects. Real defects will be considered to lie somewhere between these two extremes. The defects create strains in the lattice which, according to equation

(2), cause variations in the resonance parameter β. The extent of this variation depends on the class of defect.

An idealised point defect is taken to be localised so that the crystal lattice is disrupted only in the immediate neighbourhood of the defect. The assumption here is that the direction of propagation of the diffracted X-ray beam remains fixed with respect to the perfect lattice. As the X-rays cross the defect, $\beta(t)$ sweeps rapidly with t over a range of values and then settles back to its unperturbed value. This has two effects in the reflectance plane. Firstly, the singular point $R_0\big(\beta(t)\big)$ rapidly changes position as t is varied across the defect causing the trajectory to momentarily spiral about another point in the complex plane. Secondly, the 'angular velocity' rapidly changes, through $\omega\big(\beta(t)\big)$, which alters the rate at which the point moves from its current trajectory. The

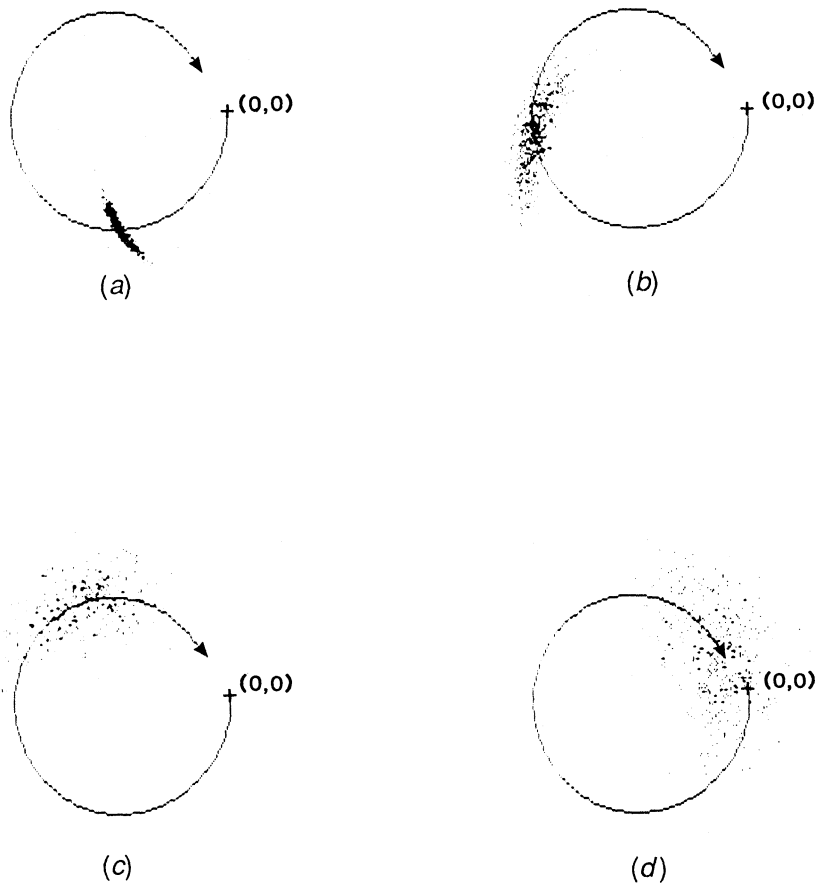

Fig. 2. Location of points in the complex plane arising from diffraction from a silicon wafer containing idealised point defects, showing the diffusion about the ideal trajectory. The reflectivity is the mean square distance of all the points from the origin. The angle of incidence of the X-rays was 9″ from the Bragg angle. Each figure is obtained for a particular thickness: (*a*) 0·5 μm, (*b*) 1·0 μm, (*c*) 1·5 μm and (*d*) 2·0 μm, where the solid line is the trajectory for a 2·0 μm thick perfect crystal.

net result is that the point in the complex plane representing the state of diffraction in the crystal momentarily deviates from its trajectory about R_0 and then continues on a neighbouring trajectory about the same singularity.

For a large ensemble of crystals with randomly distributed idealised point defects, the points in the complex plane commence along the one trajectory but begin to diffuse into the complex plane. This effect can be seen by modelling the effects of the idealised point defects using equation (7). By selecting a mean value $\bar{\beta}$, representing the perfect crystal, and introducing a random value β_ξ over a small random distance δt at random intervals, the position of a point in the complex plane can be computed for any given depth. This is repeated many times to obtain the distribution of points for the ensemble of crystals. Fig. 2 shows the distribution of points at a number of depths t for a 2 μm thick silicon 111 wafer. The solid line is the trajectory that would be followed in a perfect crystal. The diffusion of points is clearly seen although the points remain clustered about the trajectory of the ideal crystal. Note that the diffusion occurs azimuthally about the origin, rather than radially, which is to be expected since the defects randomise the phase of the X-rays. The orientation of the cluster changes as it moves along the trajectory so that the diffusion occurs along different directions with respect to the cluster. This effect reduces the anisotropy observed in Fig. 2*a*.

Extended defects may be considered within an idealised block model whereby the crystal consists of grains, or mosaic blocks, with each grain being a perfect crystal, but which may contain a constant strain, or a tilt, relative to other grains. Across a grain boundary, the state of strain changes rapidly from one value to some other, after which it is constant until the next grain boundary. In this case it is the gradient $\mathrm{d}\beta(t)/\mathrm{d}t$, which assumes a large value at the boundary and which is zero on either side of the boundary. If the resonance parameter has the values $\beta(t-\delta t)$ and $\beta(t+\delta t)$ on either side of the grain boundary at t, then the corresponding points at (x, y) in the complex plane on the trajectory about $R_0\big(\beta(t-\delta t)\big)$ will follow a new trajectory about $R_0\big(\beta(t+\delta t)\big)$. This causes all points within any cluster to diverge away from the cluster. This behaviour should also occur when a point defect causes the diffracted beam to change its direction of propagation relative to the perfect lattice.

As with idealised point defects, the effects of extended defects on the trajectories in the complex plane can be observed using equation (7). A mean value $\bar{\beta}$ is chosen and a random change in β_ξ at random intervals is introduced to compute the location of each point at a given depth. Fig. 3 shows the distribution of points for the 2 μm thick silicon 111 wafer at the same depths as in Fig. 2. Again the points diffuse from the ideal trajectory but, as discussed above, points are no longer clustered about the trajectory of the perfect crystal and they tend to diffuse over large areas in the reflectance plane.

4. Stochastic Defect Model

In the previous section it was argued that crystal defects cause the diffusion of points into the complex reflectance plane and this was demonstrated using a computer simulation based on a simple defect model. A natural extension of this model for a very large ensemble of crystals is to consider the *density* of points in the complex plane and to derive an equation governing the evolution of the density.

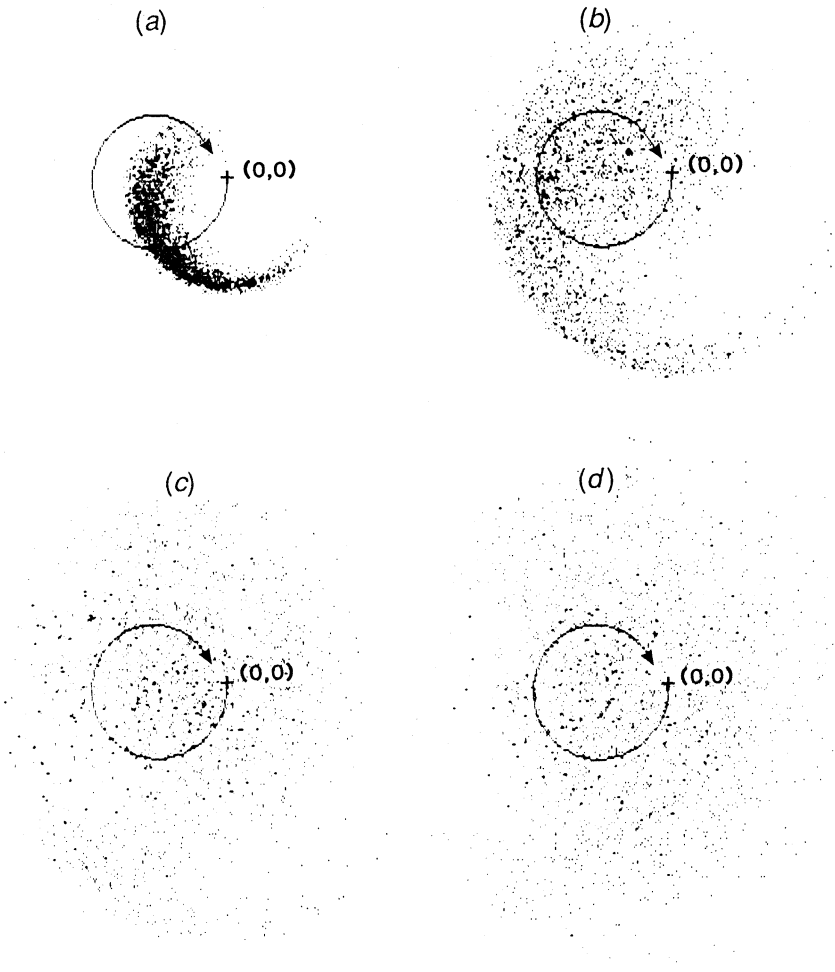

Fig. 3. Location of points in the complex plane arising from diffraction from a silicon wafer containing extended defects. As in Fig. 2, the angle of incidence of the X-rays was 9″ from the Bragg angle. Each figure is obtained for a particular thickness: (*a*) 0·5 μm, (*b*) 1·0 μm, (*c*) 1·5 μm and (*d*) 2·0 μm, where the solid line is the trajectory for a 2·0 μm thick perfect crystal.

Before this can be done, a precise mathematical statement of the defect model is required. The real, imperfect crystal is represented by an ensemble of crystals, as discussed previously, and it will be assumed that at any depth t within the real imperfect crystal, the random parameter β_ξ is gaussian distributed with a zero mean over the horizontal plane at t and that the X-ray beam is chosen with a cross section large enough to sample a significant proportion of these parameters; i.e. there is no bias in the sampling. Both defect types discussed in Section 3 were associated with an 'impulse' causing a momentary change in β, in the case of idealised point defects, and in $d\beta/dt$, in the case of extended defects. This impulse is characterised by a very short spatial extent, i.e. it is correlated only over a very short distance in

the crystal. Let the random impulse at t for one crystal within the ensemble be represented by $\xi(t)$. The parameter $\xi(t)$ is gaussian distributed over the horizontal planes at t for the crystal ensemble and it has a zero mean and a delta function autocorrelation,

$$\langle \xi(t_1)\, \xi(t_2) \rangle = \delta(t_1 - t_2). \tag{8}$$

A direct application of the Wiener–Khintchine theorem to equation (8) shows that this random term ξ has a constant spectral density, i.e. it has a 'white noise' spectrum.

Although in Section 3 the extremes of defect types were considered, namely idealised point defects and extended defects, a real crystal will contain a range of defects lying somewhere between these extremes. Also, a real point defect produces a strain field which extends into regions well away from the defect centre. This suggests the following linear combination of terms,

$$\ell(\mathrm{d}\beta_\xi/\mathrm{d}t) + \beta_\xi = \sigma\xi, \tag{9}$$

where the parameters σ and ℓ collectively determine the defect 'strength' and the similarity of the defect to the two extreme defect types. This is a stochastic differential equation and it is known as the Langevin equation (Van Kampen 1976; Risken 1984). It has been used in the study of Brownian motion (Uhlenbeck and Ornstein 1930) and it is one of the few stochastic differential equations that can be solved explicitly. With the boundary condition $\beta_\xi(t{=}0) = 0$, the solution to equation (9) is

$$\beta_\xi(t) = (\sigma/\ell) \exp(-t/\ell) \int_0^t \xi(t') \exp(t'/\ell)\, \mathrm{d}t'. \tag{10}$$

The correlation function for β_ξ can be found using equations (8) and (10):

$$\begin{aligned} \langle \beta_\xi(t_1)\, \beta_\xi(t_2) \rangle &= (\sigma/\ell)^2\, \mathrm{e}^{-(t_1+t_2)/\ell} \int_0^{t_1} \int_0^{t_2} \mathrm{e}^{(t+t')/\ell} \delta(t-t')\, \mathrm{d}t\, \mathrm{d}t' \\ &= (\sigma^2/2\ell)(\mathrm{e}^{-|t_1-t_2|/\ell} - \mathrm{e}^{-(t_1+t_2)/\ell}). \end{aligned} \tag{11}$$

Equation (11) contains a 'transient' term involving $t_1{+}t_2$. This is not required in the defect model which should have a stationary defect distribution. In this case the origin of the coordinates of the solution (11) is chosen so that $t_1{+}t_2 \gg \ell$, resulting in the following correlation function:

$$\langle \beta_\xi(t)\, \beta_\xi(t+\tau) \rangle = (\sigma^2/2\ell) \exp(-|\tau|/\ell). \tag{12}$$

Note that as $\ell \to 0$, then $\langle \beta_\xi(t)\, \beta_\xi(t{+}\tau) \rangle \to \delta(\tau)$ which is the correlation function for idealised point defects. This identifies ℓ as a correlation length in the crystal representing the characteristic distance between changes of the direction of propagation of the X-ray beam relative to the perfect lattice. Furthermore, the correlation function with $\tau = 0$ is the second moment of the probability distribution for β_ξ which means that $\sigma^2/2\ell$ is the variance of the distribution. The power spectrum of β_ξ, unlike ξ, is not constant and it describes a 'coloured noise' spectrum.

A similar result to (12) was obtained by Becker and Al Haddad (1989) who assumed a gaussian joint-probability distribution. This distribution, in fact, can be obtained as the solution of the Fokker–Planck equation derived from (9) (see Section 5 below).

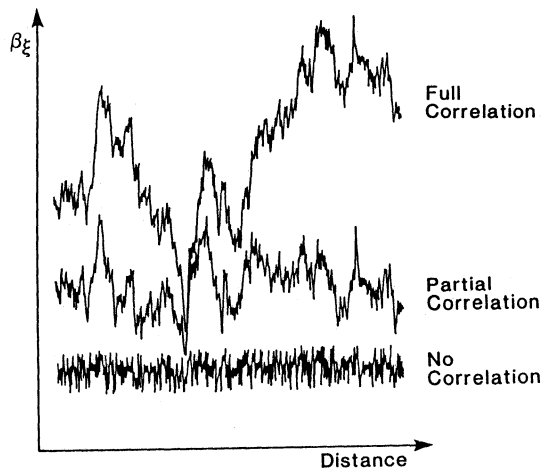

Fig. 4. An example showing the effects of the correlation length on the resonance parameter $\beta\xi$. The curves have been arbitrarily offset for clarity.

An example of the nature of $\beta\xi$ is shown in Fig. 4 where a pseudo-random number generator was used to obtain a sequence of values for $\xi = \beta\xi$ for $\ell = 0$. These values were also used with equation (10) to calculate $\beta\xi$ for the partially correlated, $\ell < \infty$, and the fully correlated, $\ell = \infty$, noise terms. Note the difference between the partially and fully correlated noise in the presence of large transients.

5. Evolution Equation for Densities in the Complex Plane

Given a first order stochastic differential equation describing the motion of points in an N-dimensional space, it is possible to write down an equation for the probability density u within that space (Van Kampen 1976; Risken 1984; Lasota and Mackey 1985). This equation is called a Fokker–Planck equation and it is obtained by the following recipe. Using the notation of Lasota and Mackey (1985), in a matrix form with the Einstein summation convention, the N-dimensional stochastic equation is

$$dx_i/dt = b_i(\boldsymbol{x}) - \sigma_{ij}(\boldsymbol{x})\,\xi_j(t), \tag{13}$$

where ξ_i is the noise term with a zero mean and a delta function autocorrelation and $1 \le i \le N$. This equation describes the dependence of the 'velocity' dx_i/dt in one dimension on all the noise terms ξ_i through the matrix σ_{ij}. The density of points $u(\boldsymbol{x})$ in the phase space with axes x_i obeys the Fokker–Planck equation

$$\partial u/\partial t = \tfrac{1}{2}(\partial^2/\partial x_i\,\partial x_j)(a_{ij}\,u) - (\partial/\partial x_i)(b_i\,u), \tag{14}$$

where

$$a_{ij}(\boldsymbol{x}) = \sigma_{ik}(\boldsymbol{x})\,\sigma_{jk}(\boldsymbol{x}). \tag{15}$$

The first term on the right side of (14) is a diffusion term which arises from the gaussian nature of the noise source. The second term represents the flow of points in the phase space driven by a 'velocity' b_i and its gradients.

The Fokker–Planck equation for the crystal reflectance is obtained by writing (1) and (9) in the form of a three-dimensional Langevin equation with dimensions (x, y, β_ξ), where $x = \mathrm{Re}\, R$ and $y = \mathrm{Im}\, R$. This requires an expansion of (1) in terms of the real and imaginary components, represented by subscripts R and I respectively,

$$\begin{aligned} \mathrm{d}x/\mathrm{d}t &= V_x(x, y, \beta_\xi), \qquad \mathrm{d}y/\mathrm{d}t = V_y(x, y, \beta_\xi), \\ \mathrm{d}\beta_\xi/\mathrm{d}t &= -\beta_\xi/\ell + (\sigma/\ell)\xi, \end{aligned} \tag{16}$$

where

$$\begin{aligned} V_x(x, y, \beta_\xi) &= -\alpha\{\chi_{hI} - 2(\bar{\beta}_R y + \bar{\beta}_I x) - 2y\beta_\xi + \chi_{-hI}(x^2 - y^2) + 2\chi_{-hR} xy\}, \\ V_y(x, y, \beta_\xi) &= \alpha\{\chi_{hR} + 2(\bar{\beta}_I y - \bar{\beta}_R x) - 2x\beta_\xi + \chi_{-hR}(x^2 - y^2) - 2\chi_{-hI} xy\}. \end{aligned} \tag{17}$$

Following the above recipe, the corresponding Fokker–Planck equation is

$$\begin{aligned} \partial u/\partial t = &-(\partial/\partial x)V_x(x, y, \beta_\xi)u - (\partial/\partial y)V_y(x, y, \beta_\xi)u \\ &+ (\partial/\partial\beta_\xi)\beta_\xi u/\ell + (\sigma^2/2\ell^2)(\partial^2/\partial\beta_\xi^2)u. \end{aligned} \tag{18}$$

This is an evolution equation for the density of points in a three-dimensional phase space, where two of the dimensions represent the complex reflectance plane while the third dimension represents all possible values of the noise term β_ξ. The solution of this equation $u(x, y, \beta_\xi, t)$ is the probability per unit volume $\mathrm{d}x\,\mathrm{d}y\,\mathrm{d}\beta_\xi$ of finding at depth t a part of the real crystal with a reflectance $R = x + \mathrm{i}y$ and a resonance parameter with a value $\bar{\beta} + \beta_\xi$. In X-ray diffraction experiments it is the mean reflectivity $\langle R^* R\rangle$ which is measured and therefore the required quantity is the second moment of the density with respect to x and y,

$$\langle R^*(t)\, R(t)\rangle = \int_{-\infty}^{\infty}\int_{-\infty}^{\infty}\int_{-\infty}^{\infty} (x^2 + y^2)u(x, y, \beta_\xi, t)\, \mathrm{d}x\, \mathrm{d}y\, \mathrm{d}\beta_\xi. \tag{19}$$

This is essentially a geometric equation which yields the mean square distance from the origin of all the points in the complex plane. The effects of imperfections on the relative phases of the X-rays is contained in the angular dependence of the density u.

In some instances [e.g. Ornstein–Uhlenbeck processes (Risken 1984)] it is possible to simplify the Fokker–Planck equation by expanding it in terms of moments, leading to equations directly involving the second and first order moments. However, such expansions are foiled by the nonlinear terms and the coupling terms $\beta_\xi x$, $\beta_\xi y$ in V_x and V_y which cause each moment to be functions of the higher order moments.

In general Fokker–Planck equations are difficult to solve and no attempt will be made here to solve (18). The fact that the equation has contained in it Riccati's equation (1), which cannot be solved explicitly in terms of quadratures, and the elementary functions of analysis for coefficients which are arbitrary functions of t (Bellman and Kalaba 1965; Brand 1966), suggests

that only approximate solutions may be obtained. This will be the subject of future investigations.

However, several observations can be made. In the absence of the 'flows' in the reflectance plane, i.e. zero gradients with respect to x and y, the equation reduces to a diffusion one for the noise density $u(\beta_\xi, t)$ and its solution, coupled with an initial condition for β_ξ gives rise to a conditional probability density $u(\beta_\xi, t|\, \beta_{\xi 0}, t_0)$. Note that the 'velocity' along the β_ξ axis is proportional $-\beta_\xi/\mathcal{L}$ so that there is a tendency for points to move towards the origin, where $\beta_\xi = 0$. This tendency of points to accumulate is balanced by the diffusion, governed by $\sigma^2/2\mathcal{L}^2$. The correlation length $\mathcal{L}$ scales the rates at which these two processes occur. This is to be expected since the correlation length determines the extent of the regions in a crystal which have similar properties and therefore must determine the rate at which the changes in β_ξ occur. When the noise term is absent, the equation merely describes the 'flow' of the points in the reflectance plane, including a term describing the change in the density due to 'velocity' gradients.

In the presence of idealised point defects, where $\mathcal{L} = 0$, the noise term $\xi = \beta_\xi$ can be included directly in equations (16). When polar coordinates are used so that $(x, y) \rightarrow (r, \theta)$ and $(V_x, V_y) \rightarrow (V_r, V_\theta)$, then the noise term decouples from the equation for $\mathrm{d}r/\mathrm{d}t$ resulting in

$$\mathrm{d}r/\mathrm{d}t = V_r(r, \theta), \qquad \mathrm{d}\theta/\mathrm{d}t = V_\theta(r, \theta) - 2\alpha\sigma\xi, \tag{20}$$

with a corresponding Fokker–Planck equation

$$\partial u/\partial t = -(\partial/\partial r)V_r u - (\partial/\partial\theta)V_\theta u + 2\alpha^2\sigma^2(\partial^2/\partial\theta^2)u. \tag{21}$$

The diffusion term is now seen explicitly in the angle coordinate θ and the points in the reflectance plane will diffuse azimuthally about the origin. This is precisely the result obtained from the simulations discussed in Section 3. This behaviour must also be described by the solutions to (18), although this is not obvious from the form of (18).

6. Discussion

It must be noted that there is a limitation with the defect model which arises from the assumed symmetrical form of the random term used to describe the defects. This is equivalent to assuming that the defects cause equal amounts of positive and negative strain in the crystal. This is true when the crystal consists mostly of randomly oriented crystal grains where the mean grain orientation is represented by $\bar{\beta}$, but it is not necessarily valid for defects which produce a bias in the strain field. For example, if there is a preponderance of interstitial atoms compared with vacancies then the bias in the strain distribution leads to an asymmetry in the X-ray scattering with angle about the Bragg angle (Dederichs 1971). This effect is essentially due to the presence of two lattice parameters, that of the unstrained regions of the lattice and that of the strained lattice due to the defects. It may be possible to model this behaviour by dividing the crystal ensemble into classes according to their average lattice parameters and calculating the probability density for each class separately. However, this would neglect any interactions between

classes. Alternatively, modifications to the Langevin equation for β_ξ may be required, possibly using a different set of statistics for ξ.

The present description of dynamical diffraction in imperfect crystals provides an alternative approach to dealing with the effects of the randomisation of the phases of the X-ray beams. A study of the behaviour of the 'flow' of points in the complex reflectance plane has led to the development of a defect model based on a stochastic differential equation. The model contains two parameters which govern the degree of imperfection of the crystal and the length scale over which changes in the crystal occur. The natural extension of this model is a Fokker–Planck equation describing the probability density of finding a particular state of the X-rays within a crystal. This provides a theoretical framework for the calculation of the diffraction intensities from imperfect crystals. While it is likely that general solutions to the Fokker–Planck equation are not possible, the geometric description of 'flows' in the complex plane provides an intuitive basis for finding approximate solutions.

Acknowledgment

The author wishes to acknowledge sponsorship from the Australian National Research Fellowship Scheme.

References

Becker, P. J., and Al Haddad, M. (1988). *Acta Cryst.* A **44**, 262–70.
Becker, P. J., and Al Haddad, M. (1989). *Acta Cryst.* A **45**, 333–7.
Bellman, R. E., and Kalaba, R. E. (1965). 'Quasilinearisation and Nonlinear Boundary Value Problems' (American Elsevier: New York).
Bogoliubov, N. N., and Mitropolsky, Y. A. (1961). 'Asymptotic Methods in the Theory of Non-linear Oscillations', Chapt. 2 (Gordon and Breach: New York).
Brand, L. (1966). 'Differential and Difference Equations' (Wiley: New York).
Dederichs, P. H. (1971). *Phys. Rev.* B **4**, 1041–50.
Holy, V. (1982). *Phys. Stat. Sol.* (*b*) **111**, 341–51.
Holy, V., and Gabrielyan, K. T. (1987). *Phys. Stat. Sol.* (*b*) **140**, 39–50.
Kato, N. (1980). *Acta Cryst.* A **36**, 763–69.
Kato, N. (1991). *Acta Cryst.* A **47**, 1–11.
Lasota, A., and Mackey, M. C. (1985). 'Probabilistic Properties of Deterministic Systems', Chapt. 11 (Cambridge Univ. Press).
Risken, H. (1984). 'The Fokker–Planck Equation: Methods of Solution and Applications' (Springer: Berlin).
Takagi, S. (1962). *Acta Cryst.* **15**, 1131.
Takagi, S. (1969). *J. Phys. Soc. Jpn* **26**, 1239–53.
Taupin, D. (1964). *Bull. Soc. Franc. Miner. Crist.* **87**, 469–511.
Uhlenbeck, G. E., and Ornstein, L. S. (1930). *Phys. Rev.* **36**, 823–41.
Van Kampen, N. G. (1976). *Phys. Reports* **24**, 171–228.

Manuscript received 6 May, accepted 7 August 1991